

# Implications of Alternative Field-Sampling Designs on Landsat-Based Mapping of Stand Age and Carbon Stocks in Oregon Forests

Maureen V. Duane, Warren B. Cohen, John L. Campbell, Tara Hudiburg, David P. Turner, and Dale L. Weyeremann

**Abstract:** Empirical models relating forest attributes to remotely sensed metrics are widespread in the literature and underpin many of our efforts to map forest structure across complex landscapes. In this study we compared empirical models relating Landsat reflectance to forest age across Oregon using two alternate sets of ground data: one from a large ( $n \sim 1500$ ) systematic forest inventory and another from a smaller set of plots ( $n < 50$ ) deliberately selected to represent pure conditions along predefined structural gradients. Models built with the smaller set of targeted ground data resulted in lower plot-level mapping error (root mean square error) and higher apparent explanatory power ( $R^2$ ) than those built with the larger, more widely distributed inventory data. However, in two of the three ecoregions considered, predictions derived from models built with the smaller ground data set displayed a bias relative to those built with the larger but noisier inventory data. A modeling exercise, wherein mapped forest age was translated into carbon, demonstrated how nonlinear ecological models can magnify these prediction biases over landscapes. From this study, it is clear that for mapping purposes, inventory data are superior to project-specific data sets if those data sets are not representative of the full region over which mapping is to be done. FOR. SCI. 56(4):405–416.

**S**PATIALLY EXPLICIT MAPS of forest biophysical variables derived from remotely sensed spectral indices are required for modeling ecosystem processes across large and heterogeneous spatial domains (Potter et al. 1993, Running and Hunt 1994, Cohen et al. 1996, Law et al. 2004, Running et al. 2004, Turner et al., 2004). When developing algorithms that convert remotely sensed spectral indices into meaningful biophysical variables, investigators often seek relationships that are based on physical principles, because these are thought to be most applicable across a range of conditions (Myneni et al. 2002). However, in most cases, empirical relationships between spectral indices and biophysical variables are developed, usually by regression analysis, from observations made at a sample of ground plots (Cohen et al. 1995, Hall et al. 2006, Lefsky et al. 1999, Means et al. 1999, Schlerf et al. 2005). The standard by which these empirical relationships are evaluated is overall goodness of fit, which is assumed to translate directly into pixel- or plot-scale accuracy across the final map product (Congalton and Green 1999). But, what if the plot samples are not representative of the whole landscape or region being mapped by spectral indices? Will there be a meaningful effect on parameter coefficients for the empirical relationships of interest? Will there be prediction biases in the regional distributions of the mapped biophysical variables? More importantly, if there are nonlinear relationships between the mapped variables (e.g., forest stand age) and an

ecological variable being modeled (e.g., biomass or carbon), what is the effect on model output? The focus of this study was to examine these questions using two separate field plot data sets collected across the forests of Oregon, USA, and a simple ecological model.

Consider a hypothetical exercise in which biological variable  $Y$  is regressed on spectral index  $X$  to map  $Y$  across a region, with the intent of using  $Y$  to drive a spatially explicit ecological model across that region. Table 1 illustrates what the true, hypothetical relationship between  $X$  and  $Y$  may look like (Equation 1) as well as two alternate relationships approximated from samples at plots (Equations 2 and 3). Equation 2 represents characteristics of the relationship derived from a relatively large number of plots placed systematically across the landscape. A large sample such as this should capture the range of variability and might, in this context, be thought of as “representative” of the mappable area. This large sample also means that Equation 2 has a poor fit (high root mean square error [RMSE]), similar to the true equation, because it contains both the error intrinsic to the relationship (as in Equation 1) and additional variance stemming from imperfect measurement. However, because the sample used to derive Equation 2 has a relatively large size (200) and captures the range of variability, estimates of the parameter coefficients ( $\beta_0$  and  $\beta_1$ ) are close to their true values. In contrast, Equation 3 was based on a small, select set of idealized ground plots chosen

---

Maureen V. Duane, Department of Forest Ecosystems and Society, 321 Richardson Hall, Oregon State University, Corvallis, OR 97331—Phone: (541) 758-8754; Fax: (541) 750-7329; maureen.duane@oregonstate.edu. Warren B. Cohen, US Forest Service—wcohen@fs.fed.us. John L. Campbell, Oregon State University—john.campbell@oregonstate.edu. Tara Hudiburg, Oregon State University—tara.hudiburg@oregonstate.edu. David P. Turner, Oregon State University—david.turner@oregonstate.edu. Dale L. Weyeremann, US Forest Service—dweyeremann@fs.fed.us.

Acknowledgments: We acknowledge the Forest Inventory and Analysis (FIA) Research Program of the US Forest Service for making available confidential FIA plot data and Elizabeth LaPoint (FIA Northern Research Station) for providing data support. We also thank Manuela Huso and Lisa Ganio for statistical consulting and guidance. Matt Gregory, Dirk Pflugmacher, and Robert Kennedy provided much needed programming skills, advice, and assistance. Zhiqiang Yang assisted with the conceptualization of the spectral variable distance<sub>bg</sub>. This research was supported by the Office of Science (BER), US Department of Energy (Grant ER64360 and ER64361).

---

Manuscript received August 13, 2009, accepted February 22, 2010

This article was written by U.S. Government employees and is therefore in the public domain.

**Table 1. Hypothetical equations describing the linear relationship between a measurable biological metric  $Y$  and a mappable spectral index  $X$  where  $Y = \beta_0 + \beta_1 X + e$**

Equation	Derivation	$n$	$\beta_0$	$\beta_1$	RMSE
1	Truth	NA	100	0.25	High
2	Modeled from large, representative sample	200	107	0.22	Higher
3	Modeled from small, idealized sample	20	185	0.12	Low

NA, not applicable.

to express pure condition classes, with minimal influence of confounding factors. Not surprisingly, this is commonly the case when plots are selected by ecologists seeking to maximize hypothesis testing power and to understand ecological processes or for ecosystem process model parameterization (Schlerf et al. 2005, Law et al. 2006). A sample such as this may be called “representative” of a predefined, select condition in a region yet “nonrepresentative” of the region as a whole because of deliberate exclusion of other condition types deemed irrelevant to the ecological questions being asked. As suggested by Equation 3, the use of idealized ground plots can lead to better fits between  $X$  and  $Y$ , but estimating the true parameter coefficients may be difficult, given that the samples are not representative of the population. We can presume that choosing Equation 3 over Equation 2 to map biological variable  $Y$  would result in a prediction bias across the mapped region. Moreover, when that variable is used in a nonlinear ecological model, the modeled output may have meaningful distributional biases that lead not only to local inaccuracies but also to large-scale biases in the modeled process over the mapped area.

Most studies relate forest biophysical variables to remote sensing spectral data using restricted data sets (Equation 3). However, examples of mapping biophysical variables with data similar to Equation 2 above exist in the literature. Large, systematically sampled data sets (as in Equation 2) are usually those collected for national-level forest inventories (Bechtold and Scott 2005). Most frequently, forest inventory data are used in conjunction with Landsat image data and nearest neighbor mapping techniques such as gradient nearest neighbor (Ohmann and Gregory 2002),  $k$ -nearest neighbor (Tomppo 1990, Tomppo and Halme 2004, Huiyan et al. 2006), or most similar neighbor (Moeur and Stage 1995) to produce multivariate maps of forest biophysical characteristics associated with vegetation class and stand age. Whereas most nearest neighbor mapping techniques adequately represent the field-based distributions of estimated variables across the mapped landscape, they commonly do so at the expense of pixel- or plot-level accuracy (McRoberts and Tomppo 2007). Another example of use of inventory data sets for mapping is the US Forest Service biomass map (Blackard et al. 2008). In that study, classification and regression trees were used to map biomass at a national scale using MODIS imagery and several ancillary data sets. The result was low local accuracy but relatively high accuracy across whole states, regions, and the nation.

In contrast to inventory-based data sets (Equation 2), most studies relate forest biophysical variables to remote sensing spectral data using restricted data sets (Equation 3). These are commonly collected for a given study and are used either to examine the potential to map biophysical

variables of interest or understand ecological processes as the primary goal, with mapping as a secondary goal. These studies usually focus much attention on the strength of empirical relationships between spectral properties and forest variables of interest, with the goal of reducing prediction error (RMSE) and maximizing predictive power ( $R^2$ ). The restricted data sets often do not represent populations of interest.

The remote sensing literature is replete with Equation 3-type examples, even if we limit our review of the literature to those studies that primarily use Landsat imagery (Cohen and Spies 1992, Kimes et al. 1996, Nelson et al. 2000, Wulder et al. 2004, Lefsky et al. 2005). Application of these equations across a broad scale and examination of regionwide distributions of the biophysical variables have received only minimal attention (Lefsky et al. 1999, Schlerf et al. 2005, Hall et al. 2006, Pflugmacher et al. 2008). Moreover, even in studies in which biophysical variables were ingested by ecosystem models (e.g., Cohen et al. 1996, Running et al. 2004, Turner et al. 2007), errors in model predictions associated with the mapped biophysical variables are rarely examined. In this article, we examine error propagation when mapping equations are applied at a regional scale and then used by an ecosystem process model to predict an important biophysical variable.

We compare the outcomes of two different plot-level data sets used to map forest stand age with Landsat imagery in Oregon, USA. Furthermore, we examine the regional effects of derived age maps for ecological modeling, using a simple nonlinear function that describes the relationship between age and carbon contained in aboveground live biomass. The first data set comes from the US Forest Service Forest Inventory and Analysis (FIA) program (Bechtold and Scott 2005). FIA collects data at a large number of ground plots (>4,000 in Oregon), systematically placed to represent the full range of forest conditions in each state of the United States.

The second data set was collected as part of a regional carbon dynamics study in Oregon and northern California (ORCA) (Hudiburg et al. 2009). The ORCA study collected data at a smaller number of ground plots, deliberately stratified across climatic space (which typically covaried with forest composition) and a remotely sensed spectral index that was known to covary with forest age and structure across western Oregon (Cohen et al. 2001). Most importantly, the ORCA study plots had to meet minimum requirements of structural homogeneity and have no indications of complex disturbance history. These selection criteria, judged subjectively through expert field reconnaissance,

ensured that plots were appropriately representative of conditions deemed a priori as ecologically important and or management relevant.

In the study reported here, our objectives were to (1) determine how well each field data set represented the bioclimatic space over which an age map was to be produced, (2) determine how the two age data sets differed in terms of their relationships with Landsat spectral indices through comparison of regression statistics, (3) assess differences in the distributions of predicted ages from applications of the regression models across our study site, and (4) examine the implications of using the age predictions derived from each data set to drive a simple, nonlinear regional carbon model.

## Methods

### Study Area

Our study area consists of three distinct ecoregions within the state of Oregon, USA: Blue Mountains, Coast Range, and East Cascades (Figure 1). Ecoregion boundaries are derived from the US Environmental Protection Agency Level III Omernik classification scheme (Omernik 1987) and delineate areas of similar biotic and abiotic characteristics, land cover, climate, soils, and topography. These

three ecoregions are situated along an east-to-west cross-section of Oregon's forest conditions. The wet, maritime Coast Range ecoregion is dominated by highly productive Douglas-fir and western hemlock forests, which are intensively managed (Franklin and Dyrness 1973). In the rain shadow of the Cascade Mountains, open stands of ponderosa and lodgepole pine, more adapted to temperature and moisture extremes, characterize the vegetation of the East Cascades ecoregion (Franklin and Dyrness 1973). Further to the east, the Blue Mountains ecoregion comprises several smaller mountain ranges mostly volcanic in origin. Vegetation in the Blue Mountains varies from open stands of ponderosa pine and Douglas-fir with dense understory at lower elevations to moderately productive spruce and fir located at higher elevations (Thorson et al. 2003).

### Plot Data

The plot data we compared in this study came from two different sources: the US Forest Service FIA program and the supplemental ground data collected specifically for ORCA-related projects (Figure 1). Both the FIA and ORCA field data used in this study were collected between 2001 and 2005.

FIA conducts a systematic sample of all forestland in the

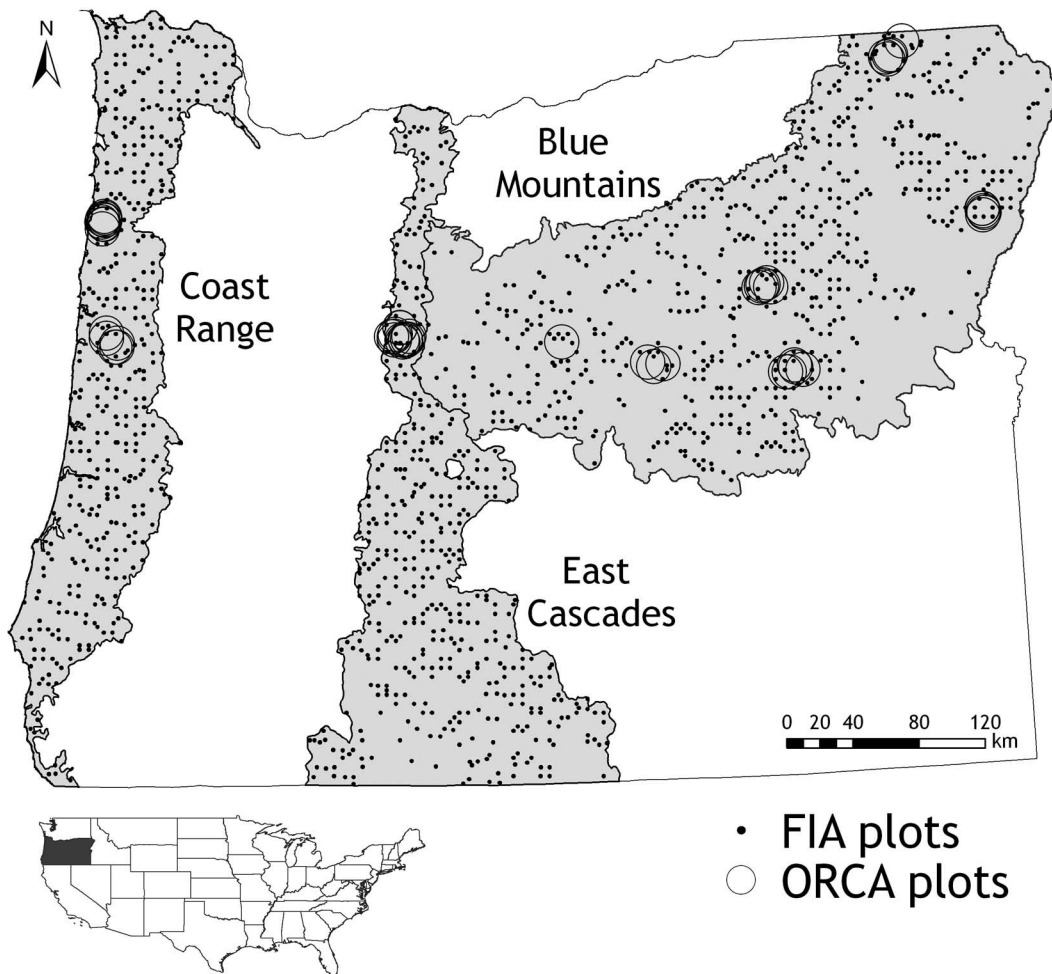


Figure 1. Distribution of plots in the Coast Range, East Cascade, and Blue Mountains ecoregions. (Differences in plot symbol size are not indicative of plot sizes but are for illustrative purposes only.)

U.S. with approximately one sample location every 2,428 ha. At each location, FIA records basic metrics necessary to assess vegetation composition, density, biomass, and growth increment over an area of 1 ha. Details regarding the FIA vegetation sampling protocol are given in Bechtold and Scott (2005). FIA assigns one or more condition classes to each plot based on differences in ownership, forest type, land use, stand size, density, or disturbance history. We used all FIA plots within our study area (1,465 in total), regardless of single or multiple conditions.

The ORCA field plots were established to augment FIA plots (Van Tuyl et al. 2005, Law et al. 2006, Hudiburg et al. 2009). In addition to the standard vegetation measurements collected at the FIA plots, the 1-ha ORCA plots received measurements pertaining to foliage, soil, and fine roots to facilitate a more comprehensive assessment of the carbon stocks and fluxes. Details regarding the ORCA vegetation sampling protocol are given in Law et al. (2006). Unlike the systematically collected FIA plots, the ORCA plots were selected to represent conditions deemed a priori as ecologically important, and logistical constraints required spatial clustering within each ecoregion (Figure 1). A total of 49 ORCA plots were established in the ecoregions of interest, all of which were used in this study. We recognize that the number of ORCA plots amounts to a fraction of the FIA plot sample size, but it was expected that they would be used either independently or in conjunction with the FIA data to map stand age.

For both data sets, wood increment data collected on live trees were used to calculate stand age for each plot. Stand age was estimated as the mean age of the oldest 10% of measured trees as described by Van Tuyl et al. (2005). Based on Spies and Franklin (1991), this method defines stand age as time since the last stand replacing disturbance, as required by ecosystem process models such as BiomeBGC (Turner et al. 2007). If there were fewer than three trees in the oldest 10%, a mean of all aged trees on the plot was used.

### *Spatial Data*

For our analyses, we assembled a suite of regression predictor and ancillary variables, including land cover, digital elevation model, and Landsat data, all resampled to a 25-m resolution. Land cover, used to stratify forest and nonforest (excluded from this study), was derived from two sources. For western Oregon (which includes the Coast Range and East Cascades ecoregions), we used a map first produced using 1988 Landsat imagery by Cohen et al. (2001) and updated to conditions in 2000 as detailed in Law et al. (2006). For eastern Oregon (including the Blue Mountains), land cover was derived solely from the 1992 National Land Cover Data map (NLCD) (Vogelmann et al. 2001). NLCD 2001 (Homer et al. 2007) was not available when this study began.

A 30-m digital elevation model for the study area was acquired from the US Geological Survey National Elevation Dataset (US Geological Survey 2006). After resampling to 25 m, we calculated slope (degrees) and aspect (0–360°). Slope, aspect, and elevation correlate to moisture and tem-

perature gradients and were used previously as proxies for bioclimatic conditions of our study area (Ohmann and Gregory 2002, Schroeder et al. 2007). In this study, these were examined as possible predictor variables and for evaluation purposes.

Peak growing season Landsat ETM+ imagery from 2000 was acquired from the Landsat Ecosystem Disturbance Adaptive Processing System (LEDAPS) project (Masek et al. 2008). All LEDAPS data were georectified and atmospherically corrected. Within an ecoregion, inter-scene radiometric normalization was performed (Cohen et al. 2001), given our ecoregion-level (as opposed to scene-level) focus and a desire to develop a single model for each ecoregion. The Landsat reflectance data were transformed into Tasseled Cap brightness, greenness, and wetness (Crist 1985, Cohen et al. 2003a) and a novel transformation called  $\text{distance}_{\text{bg}}$ , where  $\text{distance}_{\text{bg}} = \sqrt{(\text{greenness}^2 + \text{brightness}^2)}$ . For each plot, we extracted the mean and SD from all spatial data layers except land cover, for which the majority value was used. To accomplish this, a 13-pixel mask centered on the plot was used, as in related studies (Ohmann and Gregory 2002, Schroeder et al. 2007).

### *Regression Modeling*

Commonly, where the goal is to predict forest biophysical variables using remote sensing, the best predictive model is selected using established criteria (Kimes et al. 1996, Cohen et al. 2003a, Wulder et al. 2004, Parmenter et al. 2003, Schroeder et al. 2007). In this study, we explored a variety of model formulations for each ecoregion using both data sets and found that, in most cases, multiple regression models (including spectral variables and other spatial data) did not substantively reduce prediction error relative to simple linear regression based on spectral data alone. Moreover, our goal was not to derive the best predictive model; rather, it was to compare models based on data sets derived from two different sampling designs. As such, we decided to use the same, single predictor variable for all models, based on an examination of scatter plots of candidate predictors versus forest stand age (Figure 2). The natural log (ln) transformation was applied to stand age to achieve linearity. To be chosen, the predictor variable had to be nearly the best predictor for both the ORCA and FIA data sets. In this context,  $\text{distance}_{\text{bg}}$  provided the best simple linear model and was chosen for all models.

For the two field data sets, we examined whether stratification by ecoregion and/or aspect was required. Based on significance of differences between regression slopes we determined that stratification by ecoregion was warranted, but stratification by aspect was not. Six simple linear regression models were developed: one for each field data set for each of three ecoregions. To preserve the variance from the observations in the predictions, an orthogonal regression method called reduced major axis (RMA) was used (as detailed in Cohen et al. 2003a).

RMA models were applied to the spectral data for each ecoregion. For validation purposes, 20% of the FIA plots were randomly chosen and withheld from model development for use in model error assessment (for both FIA- and

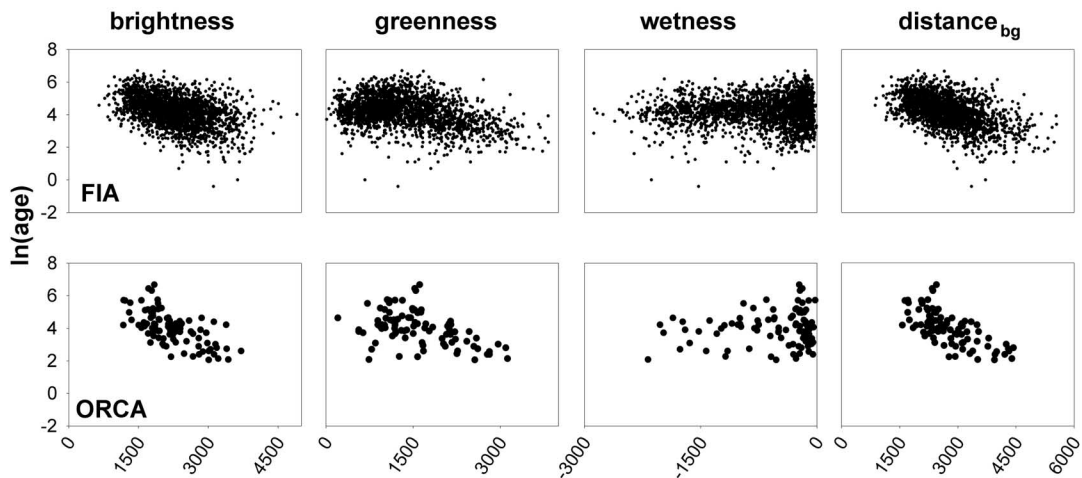


Figure 2. Scatter plots used to examine the relationship of potential spectral predictor variables with log-transformed stand age. Data from all three ecoregions are combined.

ORCA-derived models). Values for correlation ( $R$ ), RMSE, and normalized RMSE (RMSE as a percentage of the observed range) were calculated from the validation data set, as well as bias and variance ratio. Cohen et al. (2003a) described bias as the mean of predicted values minus the mean of observed values. Thus, a mean overprediction would exhibit a positive bias and vice versa. Variance ratio is calculated by dividing the SD of predicted values by the SD of observed values (Cohen et al. 2003a). Ratios  $>1$  indicate a prediction variance greater than the observed variance and vice versa. Further comparison of model predictions was based on examination of cumulative frequency histograms, by ecoregion.

### Carbon Modeling

We assessed the potential consequences of using alternate forest age maps (derived from alternate field data sets) to drive ecological models by developing simple sigmoid functions that predict carbon stored in aboveground live biomass from forest age for each of the three ecoregions (Equations 4–6 below). These functions were then applied to each of the forest age maps to generate alternate carbon mass maps from which we examined differences in frequency distributions as well as total carbon predicted from each field data set. Equations 4–6 were generated from the process model Biome-BGC that, among other outputs, simulates aboveground carbon mass throughout forest development based on inputs relating to forest type and edaphocli-

matic conditions. Equations 4–6 represent the best-fit, three-parameter Chapman (sigmoid) functions fit to forest growth simulated by Biome-BGC at 18 random forest locations in each ecoregion. The overall accuracy of these simple equations is not especially important for the needs of this study as long as they capture realistic nonlinearity between age and biomass. For details regarding the parameterization of Biome-BGC see Turner et al. (2007).

$$\text{Blue Mountains: } y = 17.20(1 - e^{-0.0078x})^{1.1657} \quad (4)$$

$$\text{Coast range: } y = 24.38(1 - e^{-0.0266x})^{2.9177} \quad (5)$$

$$\text{East Cascades: } y = 9.40(1 - e^{-0.0192x})^{1.3276} \quad (6)$$

where  $y$  is aboveground carbon ( $\text{kg C/m}^2$ ) and  $x$  is age (years).

## Results

### Representativeness of Plot Data Sets

Age distributions for the two data sets differed widely (Table 2), as expected, given the divergent sample designs and sizes. The most obvious differences were the maximum ages sampled in the Blue Mountains and Coast Range. Compared with the FIA data set, which was expected to be more representative of the true population, the ORCA data set was more representative of younger stands in the Blue Mountains and older stands in the Coast Range and East Cascades.

Table 2. Summary of plot-level data for age (in years), by ecoregion, for both field data sets

	$n$	Mean	Median	SD	Minimum	Maximum
Blue Mountains						
FIA	644	100	80	72.2	0	511
ORCA	23	72	66	33.6	34	172
Coast Range						
FIA	390	51	33	64.8	0	668
ORCA	14	66	37	65.9	8	184
East Cascades						
FIA	422	86	71	60.5	1	325
ORCA	12	108	90	95.7	8	315

The two data sets also varied in terms of their bioclimatic representativeness (Figure 3). For slope and elevation, the FIA data sets very closely matched the true distributions. This finding is expected, given that FIA is a large sample arrayed on a systematic grid. In contrast, the ORCA plots were located almost exclusively in the lower elevations of the East Cascades and in the middle elevations of the Blue Mountains (and to a lesser extent in the Coast Range). Similarly, the ORCA plots were almost exclusively on the flattest terrain in the East Cascades and the Coast Range.

It is of primary importance to examine the extent to which the spectral variable  $distance_{bg}$  was sampled across each ecoregion, given that this variable was used to model age. For the ORCA data set, the high and low ends of  $distance_{bg}$  were not well represented in the Coast Range and the low end was not sampled in the East Cascades. For the Blue Mountains, the  $distance_{bg}$  population is better sampled. Again, as expected, the FIA data set was well representative of  $distance_{bg}$ .

### Regression Models of Forest Age

Regression results between forest age (as determined from ground sampling) and remotely sensed reflectance ( $distance_{bg}$ ) reveal important differences between the FIA and ORCA field plot data sets (Table 3). Given that ORCA plots were selected to represent specific ideal conditions along a set of chronosequences, it is not surprising that data from these plots exhibit a stronger relationship of age to  $distance_{bg}$ . The differences among the regression equations

associated with the two data sets are most pronounced in the  $R^2$  values. Regardless of data set, it is clear that age and  $distance_{bg}$  are not strongly related in the Blue Mountains, whereas the strength of the ORCA age models for the Coast Range and East Cascades is almost unprecedented in the literature.

Validation statistics were calculated using the 20% of the FIA plots withheld from model development (Table 3). Values for  $R$  are very similar for both data sets in all three ecoregions, as well as RMSE for the Blue Mountains and Coast Range ecoregions. In the East Cascades, however, the RMSE of the ORCA model is more than 3 times as large as that of the FIA model. Bias values, a measure of the model's tendency toward over- or underprediction (positive and negative values respectively), varied greatly. The two Coast Range models had very similar overall model prediction bias, whereas bias was orders of magnitude larger for the ORCA models in the Blue Mountains and East Cascades.

Variance ratios were the same for the two Coast Range models and were approximately 1.0 (indicating that the models' prediction variances for age were nearly equal to the observed variances). Variance ratios for the other two FIA models were close to 1.0. For the Blue Mountains ORCA model, the variance of predicted age was less than one-half that of the observed values. The East Cascades ORCA model resulted in predictions that had a variance more than three times as large as observed values.

Normalized RMSE values were all less than 25% for the three FIA models and for two of the ORCA models. For the

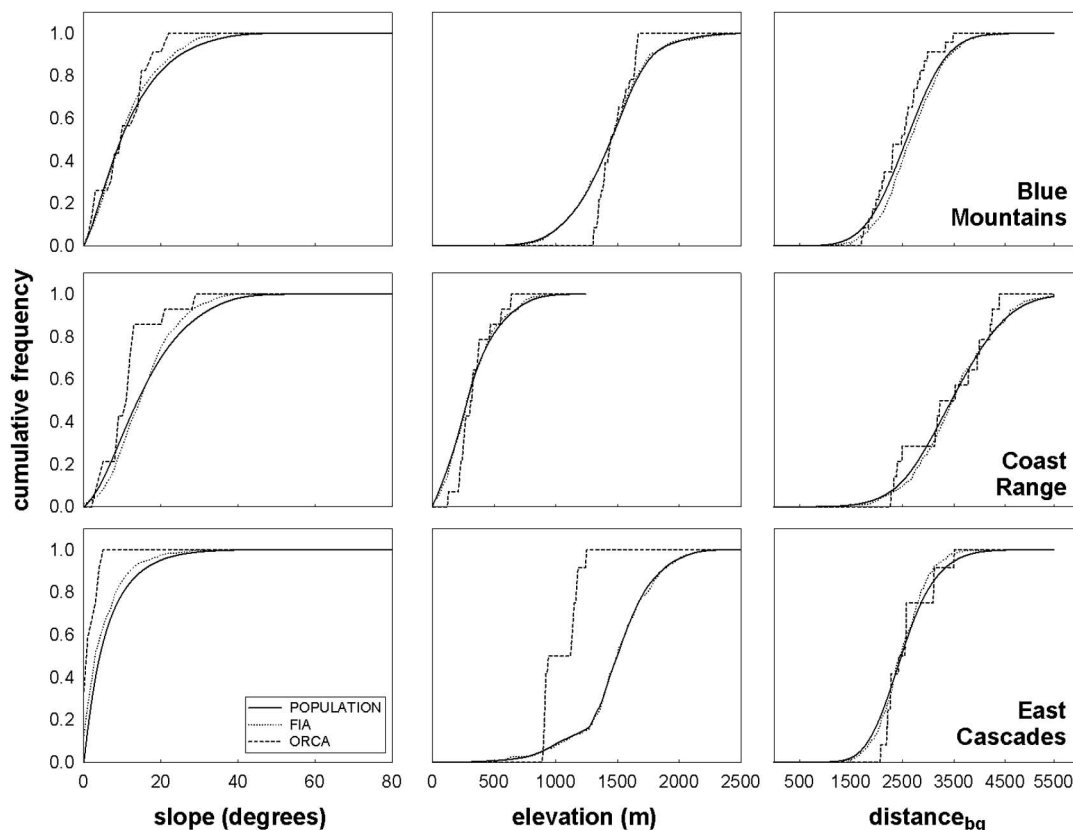


Figure 3. Cumulative frequency distributions for bioclimatic variables and the spectral variable  $distance_{bg}$  from the forested population as a whole, compared with the two sample data sets.

**Table 3. Parameter coefficients and model and validation statistics for the relationship between  $\ln(\text{age})$  and  $\text{distance}_{\text{bg}}$  for each data set by ecoregion**

	Model statistics				Validation statistics					
	$\beta_0$	$\beta_1$	$R^2$	RMSE	$R$	RMSE	Bias	Variance ratio	Normalized RMSE (%)	$n$
Blue Mountains										
FIA	7.57	-0.0012	0.11	0.65	0.18	88.88	2.53	1.11	24.86	117
ORCA	6.26	-0.0008	0.06	0.41	0.20	75.85	-36.02	0.47	21.22	117
Coast Range										
FIA	7.27	-0.0011	0.23	0.75	0.33	59.07	0.20	0.96	16.08	91
ORCA	8.56	-0.0015	0.86	0.43	0.34	58.64	0.29	0.96	15.97	91
East Cascades										
FIA	7.90	-0.0015	0.14	0.65	0.47	58.08	0.21	1.01	20.52	81
ORCA	10.71	-0.0025	0.92	0.33	0.45	179.54	67.81	3.28	63.44	81

East Cascades ORCA model, however, normalized RMSE was more than 60%.

### Forest Age Mapping

Expressions of the regression models through all forested pixels of the Landsat image data afforded the most comprehensive assessment of the models in terms of their application. Forest age maps derived from the FIA and ORCA data sets revealed dramatic differences between the alternate data sets, both in terms of the spatial distributions of age (Figure 4) and the overall age distributions (Figure 5). Recalling that the Blue Mountains had the lowest validation  $R$  (Table 3), it is not surprising that both models for this ecoregion produced maps that were not well matched to the FIA plot distributions of age. According to the FIA plot data, forests of the Blue Mountains are, on average, older than those of the Coast Range, with approximately 10% of the area being more than 200 years of age. Age maps generated using FIA-derived models suggest that approximately 10% of these forests are more than 250 years old. But this is considerably closer to the plot distribution of age than is the distribution resulting from the ORCA model, which suggests that only about 5% of these forests are more than 150 years old, a significant underestimation relative to the plot distributions.

For the Coast Range, where the FIA- and ORCA-derived

models had similar validation statistics, the maps resulted in similar age distributions (Figure 5). With the FIA plot distributions as a reference, we can see that the FIA model predictions nearly matched the actual distributions of ages for this ecoregion. Predictions from the ORCA model were skewed somewhat to the high end of the FIA plot distribution, with approximately 20% of pixels mapped with ages in excess of 100 years. For the FIA map and plots, only about 10% of the area was more than 100 years old.

The East Cascades age distributions are more similar to those of the Coast Range than the Blue Mountains, in that the FIA plot and model distributions are a near-perfect match, and the ORCA model overpredicts age relative to these two (Figure 5). The FIA data and model suggest that approximately 90% of ages are less than 200 years old and nearly 100% are less than 300 years old. The ORCA model, in contrast, suggests that only 70 and 80% of forests are less than 200 and 300 years old, respectively.

### Application of Alternate Age Maps for Modeling Carbon Stocks

The summary distributions of stocks of carbon contained in aboveground live biomass reveal the implications of using alternative age maps. The Blue Mountains age distribution from the ORCA data set was skewed toward younger ages relative to those of the FIA model (Figure 5). This

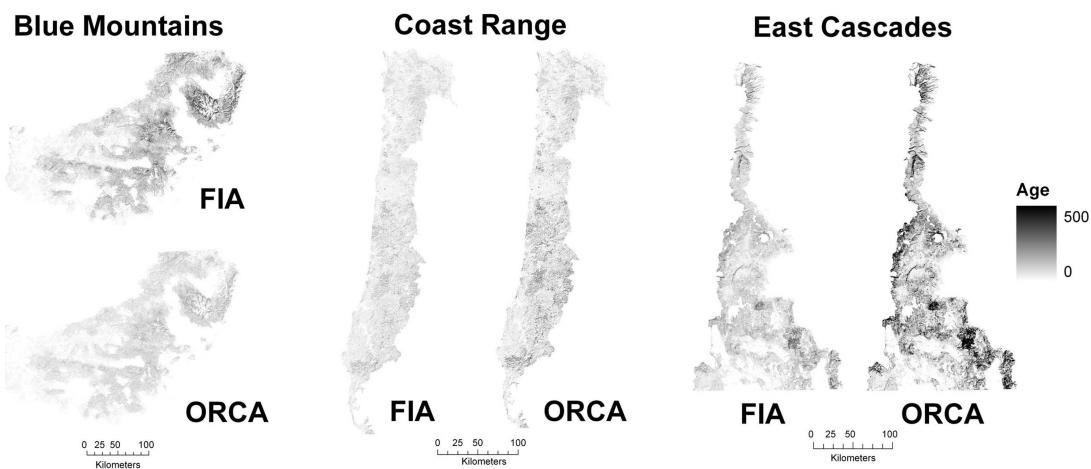


**Figure 4. Age estimates for FIA- and ORCA-derived models, all ecoregions.**

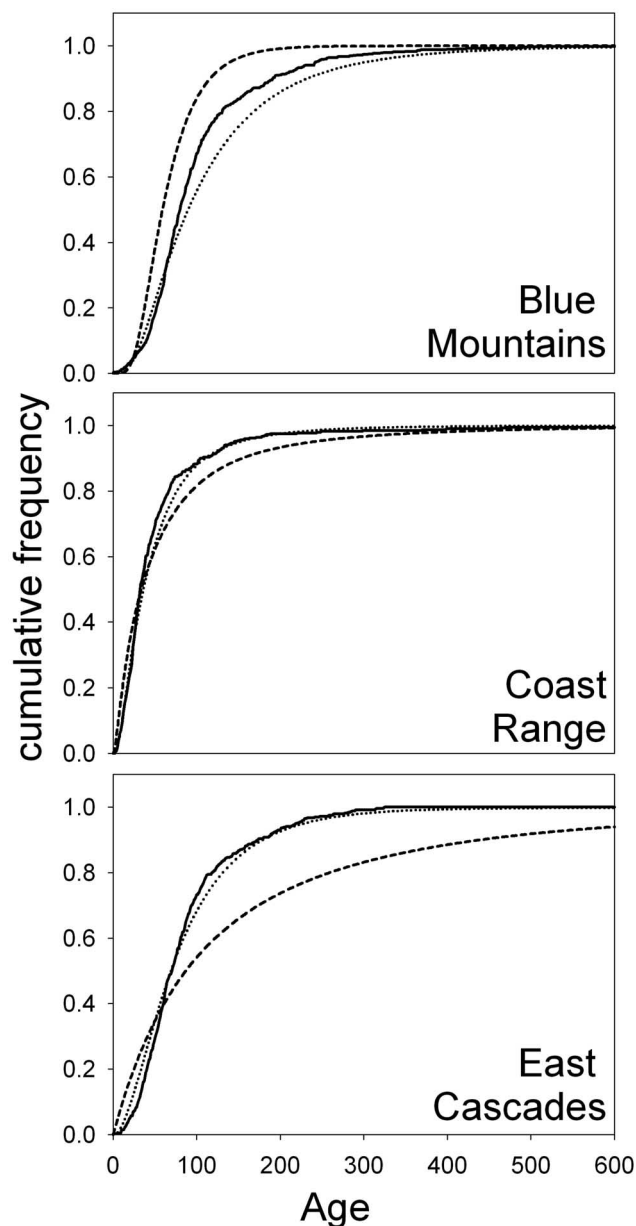


Figure 5. Cumulative frequency distributions of age estimates from FIA- and ORCA-derived models and FIA plot observed values, all ecoregions. —, FIA plot observed; ····, FIA model; ---, ORCA model.

resulted in a rather dramatic shift toward lower carbon values using the ORCA data set (Figure 6). About two-thirds of all modeled values are less than 7 kg C/m<sup>2</sup>, whereas about the same proportion are approximately 6 kg C/m<sup>2</sup> and greater, for the ORCA and FIA data sets, respectively. Consequently, the total carbon stocks resulting from each age map are very different: 164 Tg C for the ORCA map versus 231 Tg C for the FIA-derived map.

The Coast Range, which had the most similar mapped age distributions (Figure 5), also had the most similar summary carbon distributions, among the three ecoregions (Figure 6). Relative to the distributions from the FIA data set, the ORCA-based distributions are skewed slightly to the low (less than 1 kg C/m<sup>2</sup>) and high (more than 20 kg C/m<sup>2</sup>) ends. For values between 1 and 20 kg C/m<sup>2</sup>, the ORCA data set underpredicts carbon stocks relative to the FIA data set.

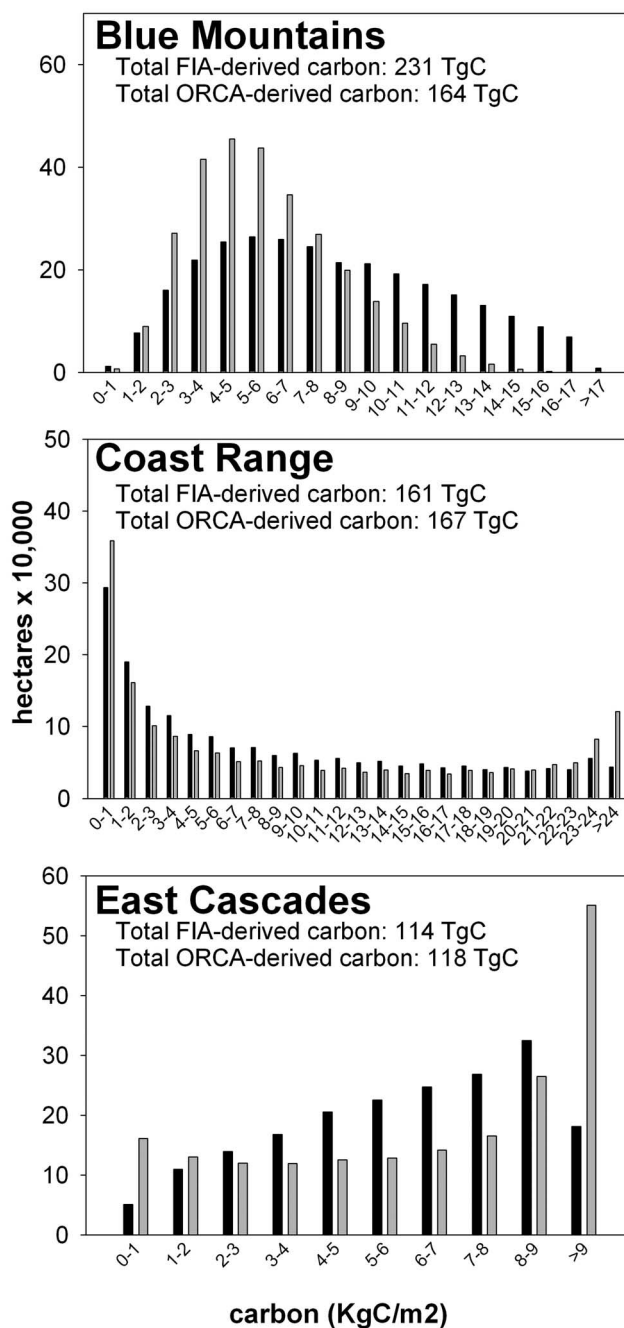


Figure 6. Distributions and totals of stocks of carbon contained in aboveground live biomass from FIA- and ORCA-derived maps, for all three ecoregions. ■, derived from FIA age map; ▒, derived from ORCA age map.

The result of both under- and overprediction is that the total amount of carbon is quite similar for both data sets: 161 Tg C versus 167 Tg C carbon.

For the East Cascades (Figure 6), the most dominant effect on carbon distributions from modeled age is the spike at the high end of the ORCA-based predictions: more than 550,000 ha are predicted to have aboveground carbon greater than 9 kg C/m<sup>2</sup>, whereas FIA-based predictions have only one-third as many hectares in that range. Again, because of compensating under- and overpredictions, total carbon for the FIA- and ORCA-derived data sets is very similar, with values of 114 and 118 Tg C, respectively.

## Discussion

This study highlights the importance of sample design when forest plot data are collected to support ecological research. Here, we demonstrate that two sets of plots, one from a systematic forest inventory data set (FIA) and the other from a focused carbon dynamics study (ORCA), can yield meaningfully different results. We focused on mapping forest age and the use of derived age maps for modeling carbon stocks.

In the remote sensing literature, plot data are often not collected with specific regard to representativeness (Lefsky et al. 1999, Cohen et al. 2003b, Schlerf et al. 2005, Hall et al. 2006). Rather, a gradient of interest is sampled, and empirical models are evaluated based on regression statistics, cross-validation, or a relatively small set of independent plots collected along the same gradient (Cohen and Spies 1992, Means et al. 1999, Lefsky et al. 2002, Cohen et al. 2003a, Law et al. 2006). This approach can be useful for exploring potential relationships between spectral data and ecological variables of interest. But as we found in our case study, how those relationships are expressed over a region when applied through a regression model is unknown and unpredictable unless the data set used to parameterize the model is representative of the region over which the model will be applied.

For example, by the standards of traditional regression statistics, the ORCA model for stand age from the East Cascades exhibited a strong relationship (Table 3). However, application of this model across the ecoregion illustrates the shortcomings of parameter estimates derived from a limited and unrepresentative sample and produces an areawide stand age distribution that is inaccurate and unrealistic (Figures 4 and 5). This limitation is related to the fact that the ORCA East Cascades plots were very limited in geographic distribution (Figure 1) and were designed specifically to sample across an age, vegetation, and climatic gradient (Law et al. 2006) rather than comprehensively sample the range of variation within the ecoregion.

In contrast, the ORCA plots in the Blue Mountains and Coast Range ecoregions, although still limited in number, had a greater geographic distribution (Figure 1) and subsequently did a better job of sampling the biogeoclimatic space across which the model was applied (Figure 3). Although these two ecoregions have noisier models (Table 3), distributions of age estimates are more realistic and match more closely those of the FIA ground plots (Figure 5).

ORCA plots are more numerous and widely distributed in the Blue Mountains (compared with the Coast Range), but the age to distance<sub>bg</sub> relationship is not strong there. This may be due more to forest stand conditions than to the sampling design. Whereas the Coast Range is dominated by even-aged, closed-canopy conifer forests where age mapping has been done previously with some success (Cohen et al. 2001), the mixture of vegetation types and age classes in the Blue Mountains (Thorson et al. 2003) makes age mapping difficult, regardless of plot distribution and representativeness.

Given an initial mapping error associated with unrepresentative samples, this error will propagate when mapped

values are used in subsequent analyses. We examined one such consequence by applying a nonlinear model to estimate carbon from modeled age. In the Blue Mountains, slight differences in age model parameters derived from the two data sets (Table 3) resulted in slightly different distributions and very different totals of aboveground carbon (Figure 6). In contrast, East Cascade age models derived from the two data sets were very different (Table 3), which resulted in very different distributions of estimated carbon (Figure 6). Despite these large differences in the distributions of carbon, totals for the region were very similar only because of compensating errors.

Certainly, field sampling designs aimed to capture idealized forest conditions over strata of ecological importance are useful. Many, if not most, ecological investigations are designed for hypotheses testing, model structuring, and model validation. Inventory data can be used for these purposes to great advantage (Turner et al. 1995, Moisen and Frescino 2002, Van Tuyl et al. 2005, Law et al. 2006, Hudiburg 2009, Pierce et al. 2009), but the noise displayed by large unfiltered ground data, such as the FIA plot data used in this study, can often obscure sought-after ecological relationships or they may not contain the specific sets of variables that are the focus of the study (e.g., belowground carbon flux). Field data are expensive, and the costs of collecting large data sets to support mapping, when mapping is only one of many objectives, may be prohibitive. But, at the very least, in collection of field data multiple objectives need to be taken into consideration.

For mapping purposes, inventory data may also be troublesome when one is focused on minimizing plot-level mapping error. The dominant theme in the literature is maximizing plot-level predictive power (Congalton and Green 1999). Those who use inventory data recognize that relationships derived from those data are quite noisy but are focused more on using those data because they are representative of large areas over which maps are required for stratification and estimation (Ohmann and Gregory 2002, McRoberts and Tomppo 2007, Blackard et al. 2008, Pierce et al. 2009). From this study, it is clear that for mapping purposes, inventory data are superior to project-specific data sets if those data sets are not representative of the full region over which mapping is to be done. Rather than minimizing plot-level mapping error (RMSE) and maximizing explanatory power ( $R^2$ ), it is much more important for mapping studies to get the coefficients of the relationship right so that prediction biases are minimized. This is particularly important when the maps are to be used for regional modeling studies and especially when the regional models incorporate mapped variables in a nonlinear fashion, as demonstrated here.

Understanding and predicting forest processes associated with biogeochemical cycling, stand dynamics, and disease spread depend increasingly on our ability to distribute process models across diverse landscapes using available map products for model inputs. Advances in remote sensing and increases in availability of derived products provide many map choices to modelers. Understanding the accuracy of these data sets is critical but rather than focus solely on accuracy statistics, it will be important to consider more

expressly how remotely sensed maps represent the region of interest in terms of their prediction biases.

Stand age is an important variable for carbon modeling. We only focused on summary distributions of carbon contained in aboveground live biomass in this study, but there are a host of other processes for which age is critical (e.g., decomposition of aboveground woody debris after disturbance and soil respiration). Because of the nonlinear nature of the processes associated with age, even for summary distributions, the effects of biased age mapping remain unknown unless tested. Moreover, mapping the proper spatial distributions of age can be as important as getting the summary distributions right and is essential in situations for which there are steep environmental gradients and interactions between age and those gradients. Simply put, our models of carbon dynamics may result in important biases if the input map surfaces derived from remote sensing have prediction biases themselves.

The novel spectral transformation distance<sub>bg</sub> is based on an accumulated understanding of Tasseled Cap spectral space by the authors. Cohen et al. (1995) first conceptualized the temporal trajectory of conifer forest stands in western Oregon through brightness-greenness space, revealing that as closed canopy conifer forests aged they moved closer to the spectral origin. This occurs because of self-thinning and structural complexity that increase as stands age, both of which lead to increased shadow proportion in Landsat pixels. As distance<sub>bg</sub> is a direct measure of distance from the origin, we hypothesized that it would be strongly correlated to conifer stand age. We examined that relationship in this study and found our hypothesis to be true.

## Summary and Conclusions

We tested the effects of two different field sample data sets on mapping forest age with Landsat data. We then used these maps with a simple ecosystem process model to quantify aboveground carbon stocks in Oregon, USA. The data sets represent diverse perspectives on sampling, given their differing purposes and the fact that neither was designed for a primary use with remote sensing. The most important findings and conclusions from this study were the following:

- ▶ Regression model statistics do not reveal the true power of a relationship between spectral data and field-based measures such as forest age. Although high  $R^2$  and low RMSE may be valuable for determining what the best set of predictor variables might be, it is only the first step in a remote sensing application.
- ▶ We assert that for mapping applications in ecology, obtaining the proper summary frequency distributions of the mapped variable is far more important than achieving a strong relationship, as judged using regression statistics. This is best assured by designing or using a sample that is directed to capturing the variation in the full population of interest.
- ▶ Nonlinear ecosystem process models that ingest remote sensing products can have unknown and surprising results if the errors and prediction biases of these products

are not well understood. For example, we demonstrated that products derived from nonrepresentative data sets, when used with a carbon model, can result in strong biases in summary carbon distributions.

- ▶ Obtaining reliable summary distributions can come at the expense of local accuracy. The only way to understand the quality of local map accuracy is to use an independent sample that represents the full population of interest. Simply using another nonrepresentative data set sampled along a gradient of interest will not reveal the true mapping errors.
- ▶ Ecosystem modelers using remote sensing products must do so with caution and not simply accept reported error rates as truth, given that these almost always focus on local accuracy and not on summary distributions.
- ▶ Careful consideration should be given to how remote sensing products propagate error through nonlinear ecosystem models. Local accuracy and regional representation are not mutually exclusive, but unless both are explicitly considered and characterized, the true contributions of remote sensing to the total error can never be realized.

## Literature Cited

- BECHTOLD, W.A., AND C.T. SCOTT. 2005. The Forest Inventory and Analysis plot design. P. 27–42 in *The enhanced Forest Inventory and Analysis program—National sampling design and estimation procedures*, Bechtold, W.A., and P.L. Patterson (eds.). Gen. Tech. Rep. SRS-80. US For. Serv., South. Res. Stn., Asheville, NC. 85 p.
- BLACKARD, J.A., M.V. FINCO, E.H. HELMER, G.R. HOLDEN, M.L. HOPPUS, D.M. JACOBS, A.J. LISTER, G.G. MOISEN, M.D. NELSON, R. RIEMANN, B. RUEFENACHT, D. SALAJANU, D.L. WEYERMANN, K.C. WINTERBERGER, T.J. BRANDEIS, R.L. CZAPLEWSKI, R.E. MCROBERTS, P.L. PATTERSON, AND R.P. TYMCIO. 2008. Mapping U.S. forest biomass using nationwide forest inventory data and moderate resolution information. *Remote Sens. Environ.* 112(4 Spec. Issue):1658–1677.
- COHEN, W.B., M.E. HARMON, D.O. WALLIN, AND M. FIORELLA. 1996. Two decades of carbon flux from forests of the Pacific Northwest, *BioScience* 46:836–844.
- COHEN, W.B., T.K. MAIERSPERGER, S.T. GOWER, AND D.P. TURNER. 2003a. An improved strategy for regression of biophysical variables and Landsat ETM+ data. *Remote Sens. Environ.* 84:561–571.
- COHEN, W.B., T.K. MAIERSPERGER, T.A. SPIES, AND D.R. OETTER. 2001. Modeling forest cover attributes as continuous variables in a regional context with Thematic Mapper data. *Int. J. Remote Sens.* 22:2279–2310.
- COHEN, W.B., T.K. MAIERSPERGER, Z. YANG, S.T. GOWER, D.P. TURNER, W.D. RITTS, M. BERTERRETICHE, AND S.W. RUNNING. 2003b. Comparisons of land cover and LAI estimates derived from ETM+ and MODIS for four sites in North America: A quality assessment of 2000/2001 provisional MODIS products. *Remote Sens. Environ.* 88:233–255.
- COHEN, W.B., AND T.A. SPIES. 1992. Estimating structural attributes of Douglas-fir/Western hemlock forest stands from LANDSAT and SPOT imagery. *Remote Sens. Environ.* 41: 1–17.
- COHEN, W.B., T.A. SPIES, AND M. FIORELLA. 1995. Estimating the age and structure of forests in a multi-ownership landscape of western Oregon, USA. *Int. J. Remote Sens.* 16:721–746.
- CONGALTON, R. AND K. GREEN. 1999. *Assessing the accuracy of*

- remotely sensed data: Principles and practices. CRC/Lewis Press, Boca Raton, FL. 137 p.
- CRIST, E.P. 1985. A TM tasseled cap equivalent transformation for reflectance factor data. *Remote Sens. Environ.* 17:301–306.
- FRANKLIN, J.F., AND C.T. DYRNES. 1973. Natural vegetation of Oregon and Washington. Gen. Tech. Rep. PNW 8. US For. Serv. Pacific Northw. For. Range Exp. Stn.
- HALL, R.J., R.S. SKAKUN, E.J. ARSENAULT, AND B.S. CASE. 2006. Modeling forest stand structure attributes using Landsat ETM+ data: Application to mapping of aboveground biomass and stand volume. *For. Ecol. Manag.* 225(1–3):378–390.
- HOMER, C., J. DEWITZ, J. FRY, M. COAN, N. HOSSAIN, C. LARSON, N. HEROLD, A. MCKERROW, J.N. VAN DRIEL, AND J. WICKHAM. 2007. Completion of the 2001 National Land Cover Database for the conterminous United States. *Photogramm. Eng. Remote Sens.* 73:337–341.
- HUDBURG, T., B. LAW, D.P. TURNER, J.L. CAMPBELL, D. DONATO, AND M. DUANE. 2009. Carbon dynamics of Oregon and northern California forests and potential land-based carbon storage. *Ecol. Applic.* 19:163–180.
- HUIYAN, G., D. LIMIN, W. GANG, X. DONG, W. SHUNZHONG, AND W. HUI. 2006. Estimation of forest volumes by integrating Landsat TM imagery and forest inventory data. *Sci. China Ser. E Technol. Sci.* 49:54–62.
- KIMES, D.S., B.N. HOLBEN, J.E. NICKESON, AND W.A. MCKEE. 1996. Extracting forest age in a Pacific Northwest forest from Thematic Mapper and topographic data. *Remote Sens. Environ.* 56:133–140.
- LAW, B.E., D. TURNER, J. CAMPBELL, O.J. SUN, S. VAN TUYL, W.D. RITTS, AND W.B. COHEN. 2004. Disturbance and climate effects on carbon stocks and fluxes across Western Oregon USA. *Glob. Change Biol.* 10:1429–1444.
- LAW, B.E., D. TURNER, M. LEFSKY, J. CAMPBELL, M. GUZY, O. SUN, S.V. TUYL, AND W. COHEN. 2006. Carbon fluxes across regions: Observational constraints at multiple scales. P. 167–190 in *Scaling and uncertainty analysis in ecology: Methods and applications*, Wu, J., B. Jones, H. Li, and O. Loucks (eds.). Springer, USA, New York, NY.
- LEFSKY, M.A., W.B. COHEN, S.A. ACKER, G.G. PARKER, T.A. SPIES, AND D. HARDING. 1999. Lidar remote sensing of the canopy structure and biophysical properties of Douglas-fir/western hemlock forests. *Remote Sens. Environ.* 70: 339–361.
- LEFSKY, M.A., W.B. COHEN, D.J. HARDING, G.G. PARKER, S.A. ACKER, AND S.T. GOWER. 2002. Lidar remote sensing of aboveground biomass in three biomes. *Glob. Ecol. Biogeog.* 11:393–399.
- LEFSKY, M.A., D.P. TURNER, M. GUZY, AND W.B. COHEN. 2005. Combining lidar estimates of biomass and Landsat estimates of stand age for spatially extensive validation of modeled forest productivity. *Remote Sens. Environ.* 95:549–558.
- MASEK, J.G., C. HUANG, R. WOLFE, W. COHEN, F. HALL, J. KUTLER, AND P. NELSON. 2008. North American forest disturbance mapped from a decadal Landsat record. *Remote Sens. Environ.* 112:6, pp. 2914–2926.
- MCRBERTS, R.E., AND E.O. TOMPPA. 2007. Remote sensing support for national forest inventories. *Remote Sens. Environ.* 110:412–419.
- MEANS, J.E., S.A. ACKER, D.A. HARDING, J.B. BLAIR, M.A. LEFSKY, W.B. COHEN, M.E. HARMON, AND W.A. MCKEE. 1999. Use of large-footprint scanning airborne lidar to estimate forest stand characteristics in the western Cascades of Oregon. *Remote Sens. Environ.* 67:298–308.
- MOEUR, M., AND A.R. STAGE. 1995. Most similar neighbor: An improved sampling inference procedure for natural resource planning. *For. Sci.* 41:337–359.
- MOISEN, G.G., AND T.S. FRESCINO. 2002. Comparing five modeling techniques for predicting forest characteristics. *Ecol. Model.* 157:209–225.
- MYNENI, R.B., S. HOFFMAN, Y. KNYAZIKHIN, J.L. PRIVETTE, J. GLASSY, Y. TIAN, Y. WANG, X. SONG, Y. ZHANG, G.R. SMITH, A. LOTSCH, M. FRIEDL, J.T. MORISSETTE, P. VOTAVA, R.R. NEMANI, AND S.W. RUNNING. 2002. Global products of vegetation leaf area and fraction absorbed PAR from year one of MODIS data. *Remote Sens. Environ.* 83:214–231.
- NELSON, R.F., D.S. KIMES, W.A. SALAS, AND M. ROUTHIER. 2000. Secondary forest age and tropical forest biomass estimation using Thematic Mapper imagery. *BioScience* 50(5):419–431.
- OHMANN, J.L., AND M.J. GREGORY. 2002. Predictive mapping of forest composition and structure with direct gradient analysis and nearest neighbor imputation in coastal Oregon, USA. *Can. J. For. Res.* 32:725–741.
- OMERNIK, J.M. 1987. Ecoregions of the conterminous United States. Map (scale 1:7,500,000). *Ann. Assoc. Am. Geographers* 77:118–125.
- PARMENTER, A.W., A. HANSEN, R. KENNEDY, W.B. COHEN, U. LANGNER, R. LAWRENCE, B. MAXWELL, A. GALLANT, AND R. ASPINALL. 2003. Land use and land cover change in the Greater Yellowstone Ecosystem: 1975–1995. *Ecol. Applic.* 13: 687–703.
- PFLUGMACHER D, W. COHEN, R. KENNEDY, AND M. LEFSKY. 2008. Regional applicability of forest height and aboveground biomass models for the geoscience laser altimeter system. *For. Sci.* 54(6):647–657.
- PIERCE, K.B., JR., J.L. OHMANN, M.C. WIMBERLY, M.J. GREGORY, AND J.S. FRIED. 2009. Mapping wildland fuels and forest structure for land management: A comparison of nearest-neighbor imputation and other methods. *Can. J. For. Res.* 39(10): 1901–1916.
- POTTER, C.S., J.T. RANDERSON, C.B. FIELD, P.A. MATSON, P.M. VITOUSEK, H.A. MOONEY, AND S.A. KLOOSTER. 1993. Terrestrial ecosystem production: A process model based on global satellite and surface data. *Glob. Biogeochem. Cycles* 7(4):811–841.
- RUNNING, S., AND E.R. HUNT, JR. 1994. Generalization of a forest ecosystem process model for other biomes, BIOME-BGC, and an application for global scale models. P. 141–157 in *Scaling physiological processes: Leaf to globe*, Ehleringer, J., and C. Field (eds.). Academic Press, Toronto, ON, Canada.
- RUNNING, S.W., R.R. NEMANI, F.A. HEINSCH, M. ZHAO, M. REEVES, AND H.A. HASHIMOTO. 2004. Continuous satellite-derived measure of global terrestrial primary production. *BioScience* 54(6):547–560.
- SCHLERF, M., C.G. ATZBERGER, AND J. HILL. 2005. Remote sensing of forest biophysical variables using HyMap imaging spectrometer data. *Remote Sens. Environ.* 95(2):177–194.
- SCHROEDER, T.A., W.B. COHEN, AND Z. YANG. 2007. Patterns of forest regrowth following clearcutting in western Oregon as determined from a Landsat time-series. *For. Ecol. Manag.* 243:259–273.
- SPIES, T.A., AND J.F. FRANKLIN. 1991. The structure of natural young, mature, and old-growth Douglas-fir forests in Oregon and Washington. In *Wildlife habitat relationships in old-growth Douglas-fir forests*, Ruggiero, L.F., K.B. Aubry, A.B. Carey, and M.H. Huff (eds.). US For. Serv. Gen. Tech. Rep. PNW GTR-285.
- THORSON, T.D., S.A. BRYCE, D.A. LAMMERS, A.J. WOODS, J.M. OMERNIK, J. KAGAN, D.E. PATER, AND J.A. COMSTOCK. 2003. Ecoregions of Oregon [two-sided color poster with map, descriptive text, summary tables, and photographs; scale

- 1:1,350,000. U.S. Geological Survey, Reston, VA.
- TOMPPO, E. 1990. Satellite image-based national forest inventory of Finland. *Photogramm. J. Finland* 12(1):115–120.
- TOMPPO, E., AND M. HALME. 2004. Using coarse scale forest variables as ancillary information and weighting of variables in k-NN estimation: A genetic algorithm approach. *Remote Sens. Environ.* 92:1–20.
- TURNER, D.P., G.J. KOERPER, M.E. HARMON, AND J.L. JEFFREY. 1995. A carbon budget for forests of the conterminous United States. *Ecol. Applic.* 5(2):421–436.
- TURNER, D.P., S.V. OLLINGER, AND J.S. KIMBALL. 2004. Integrating remote sensing and ecosystem process models for landscape- to regional-scale analysis of the carbon cycle. *BioScience* 54(6):573–584.
- TURNER, D.P., W.D. RITTS, B.E. LAW, W.B. COHEN, Z. YANG, T. HUDIBURG, J.L. CAMPBELL, AND M.V. DUANE. 2007. Scaling net ecosystem production and net biome production over a heterogeneous region in the western United States. *Biogeosciences* 4:597–612.
- US GEOLOGICAL SURVEY. (2006) *National elevation dataset*. Available online at [ned.usgs.gov/Ned/index.asp](http://ned.usgs.gov/Ned/index.asp); last accessed Jun. 9, 2006.
- VAN TUYL S, B.E. LAW, D.P. TURNER, AND A.I. GITELMAN. 2005. Variability in net primary production and carbon storage in biomass across Oregon forests—An assessment integrating data from forest inventories, intensive sites, and remote sensing. *For. Ecol. Manag.* 209:273–291.
- VOGELMANN, J.E., S.M. HOWARD, L. YANG, C.R. LARSON, B.K. WYLIE, AND J.N. VAN DRIEL. 2001. Completion of the 1990's national land cover data set for the conterminous United States. *Photogramm. Eng. Remote Sens.* 67:650–662.
- WULDER, M.A., R.S. SKAKUN, W.A. KURZ, AND J.C. WHITE. 2004. Estimating time since forest harvest using segmented Landsat ETM+ imagery. *Remote Sens. Environ.* 93:179–187.